Ferroelectric Liquid Crystals Induced by Atropisomeric Biphenyl Dopants: Dependence of the Polarization Power on the Nature of the Symmetry-Breaking Groups

Despina Vizitiu,[†] Carmen Lazar,[†] Joshua P. Radke,[‡] C. Scott Hartley,[†] Matthew A. Glaser,[§] and Robert P. Lemieux*,[†]

Department of Chemistry, Queen's University, Kingston, Ontario, Canada K7L 3N6, and Department of Chemistry and Biochemistry and Department of Physics and Ferroelectric Liquid Crystal Materials Research Center (FLC MRC), University of Colorado, Boulder, Colorado 80309

Received September 19, 2000. Revised Manuscript Received February 16, 2001

Four new chiral dopants containing an atropisomeric biphenyl core derived from 4,4′-dihydroxy-2,2′,6,6′-tetramethylbiphenyl with different symmetry-breaking groups at the 3,3′-positions (X = F, Cl, Br, and Me) were synthesized in optically active form. These dopants were used to induce ferroelectric SmC* liquid crystal phases in four SmC hosts with different core structures. Polarization powers δ_p were measured as a function of the SmC host and compared to δ_p values previously obtained for an analogous atropisomeric dopant with X = NO_2. Theoretical conformational analyses for rotation of the atropisomeric cores about the C−O bonds of the ester groups linking the core to the side chains were performed at the B3LYP/6-31G(d) level and used in calculating Boltzmann-weighed statistical average transverse dipole moments $\langle\mu_\perp\rangle$ for the core−diester units. The $\langle\mu_\perp\rangle$ values were used to normalize δ_p to study the influence of the symmetry-breaking groups X on the polar ordering of the dopants. Variations in $\delta_{p(norm)}$ are rationalized by considering models describing either achiral or chiral distortions of the zigzag binding site model of the SmC host. Results show that the symmetry-breaking groups X exert a unique influence on polar ordering of the dopants in the phenylpyrimidine host **PhP1** that is consistent with a model in which chirality transfer via core−core interactions between dopant and host molecules causes a chiral distortion of the zigzag binding site.

Introduction

Over the past 25 years, the study of ferroelectric liquid crystals (FLC) has developed into a rich multidisciplinary science that effectively bridges the fields of organic and physical chemistry to that of condensed matter physics. In 1975, Meyer and co-workers first predicted and experimentally demonstrated that a chiral smectic C (SmC*) liquid crystal phase should exhibit polar order.[1] Subsequently, Clark and Lagerwall showed that the helical structure of a SmC* liquid crystal spontaneously unwinds between rubbed polyimide-coated glass slides to give a surface-stabilized ferroelectric liquid crystal (SSFLC) with a spontaneous polarization (P_S) oriented normal to the glass plates, along the polar C_2 axis of the SmC* phase (Figure 1).[2]

An important aspect of FLC research has focused on the relationship between the molecular structure of the chiral constituent(s) of a SmC* liquid crystal and the magnitude of P_S.[3] Commercial liquid crystal mixtures for SSFLC display applications are normally obtained by mixing a chiral dopant with high polarization power (δ_p) into an achiral SmC liquid crystal host with low viscosity and a wide temperature range. The polarization power measures the propensity of a chiral dopant to induce a spontaneous polarization according to eq 1, where x_d is the dopant mole fraction and P_o is the reduced polarization of the SmC* phase.[4] The reduced polarization is normalized for variations in tilt angle θ and is related to the spontaneous polarization P_S by eq 2.[5] Chiral dopants for FLC mixtures may or may not be mesogenic themselves, but they generally have structures similar to SmC mesogens, that is, a rigid aromatic core and two aliphatic side chains.

$$\delta_p = \left(\frac{dP_o(x_d)}{dx_d}\right)_{x_d \to 0} \quad (1)$$

$$P_o = P_S/\sin\theta \quad (2)$$

Recent studies by Stegemeyer and co-workers have examined the dependence of δ_p on the nature of the

* To whom correspondence should be addressed. E-mail: lemieux@chem.queensu.ca.
[†] Queen's University.
[‡] Department of Chemistry and Biochemistry and FLC MRC, University of Colorado.
[§] Department of Physics and FLC MRC, University of Colorado.

(1) Meyer, R. B.; Liebert, L.; Strzelecki, L.; Keller, P. *J. Phys. (Paris) Lett.* **1975**, *36*, L69.
(2) Clark, N. A.; Lagerwall, S. T. *Appl. Phys. Lett.* **1980**, *36*, 899.
(3) Walba, D. M. In *Advances in the Synthesis and Reactivity of Solids*; Mallouck, T. E., Ed.; JAI Press Ltd.: Greenwich, CT, 1991; Vol. 1, pp 173−235.
(4) Siemensmeyer, K.; Stegemeyer, H. *Chem. Phys. Lett.* **1988**, *148*, 409.

10.1021/cm000753k CCC: $20.00
Published on Web 04/05/2001

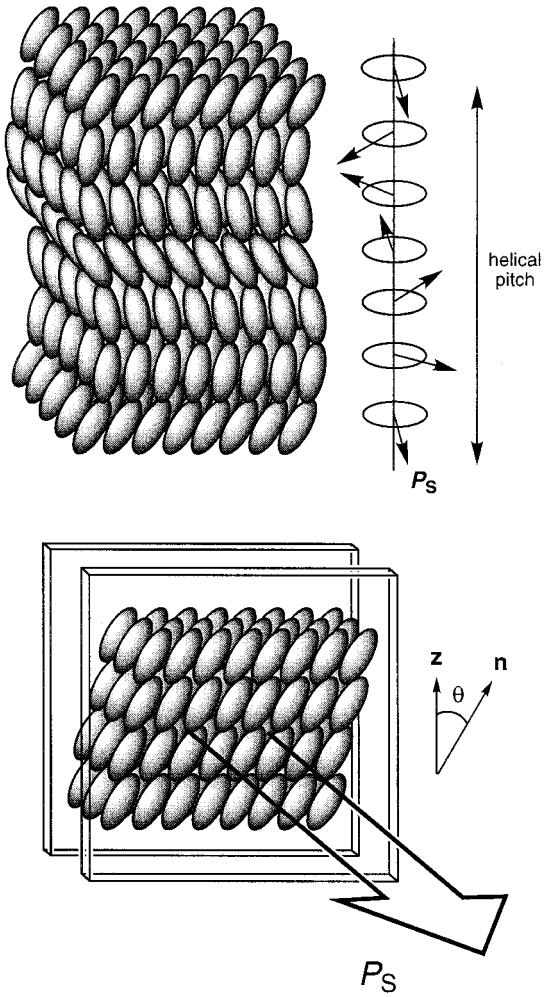

Figure 1. Schematic representations of the chiral SmC* phase as a macroscopic helix in the absence of surface alignment (top) and as a surface-stabilized FLC film between two glass slides (bottom). The vectors **z** and **n** are in the plane of the page and the polar axis is normal to the plane of the page. The sign of P_S shown in this figure is negative.

achiral SmC host.[6,7] The vast majority of chiral dopants known to induce a SmC* liquid crystal phase contain chiral side chains and generally exhibit a polarization power that does not vary significantly from one structural class of SmC host to the next (Type I). On the other hand, the polarization power of dopants with rigid chiral cores tends to vary with the structure of the SmC host (Type II). This host effect is thought to arise from rigid core−core interactions between chiral dopant and surrounding host molecules and may be viewed as a manifestation of host−guest molecular recognition that cannot be achieved with Type I dopants because of the higher degree of conformational disorder among side chains in the SmC* phase.[6,7]

We have shown that the polarization power of novel Type II dopants with an atropisomeric dinitrobiphenyl core (e.g., **1**) depends strongly on the core structure of the achiral SmC host.[8] The highest δ_p values were

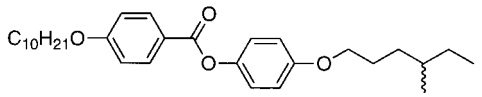

PhB; phase sequence: Cr 35 S_C 70.5 S_A 72 N 75 I

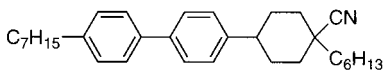

NCB76; phase sequence: Cr 66 (S_G 55) S_C 73 S_A 117 N 125 I

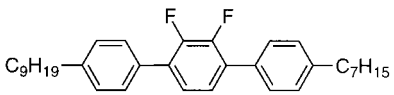

DFT; phase sequence: Cr 49 S_C 77 S_A 93 N 108 I

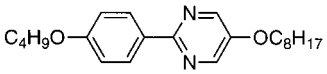

PhP1; phase sequence: Cr 58 S_C 85 S_A 95 N 98 I

Figure 2. Structures of the liquid crystal hosts and phase transition temperatures in °C.

recorded in the phenylpyrimidine host **PhP1** (Figure 2), which is a very good structural match for effective chirality transfer via core−core interactions with the dopant,[9] while the lowest δ_p values were recorded in the phenyl benzoate host **PhB**, which is a poor structural match for such interactions. Measurements of δ_p as a function of the length of the dopant side chains (n) showed that the spontaneous polarization induced in **PhP1** is uniquely sensitive to the positional ordering of the atropisomeric core with respect to the core sublayer of the SmC host. Furthermore, we showed that the helical pitch (p) of the induced SmC* phases varies with the dopant chain length n and follows a trend opposite to that observed for δ_p versus n, which suggests that chirality transfer via core−core interactions plays a significant role in the induction of high spontaneous polarizations in **PhP1**.

The polar ordering of dopants such as **1** is thought to originate from a small asymmetric bias in the energy profile for rotation of the rigid biphenyl core about the two ester C−O bonds, which results in a preferred orientation of the core transverse dipole moment along the polar axis in the SmC* phase (Figure 3).[8] According to this model, the polarization power of an atropisomeric dopant with the general core structure shown in Figure 3 should strongly depend on the nature of the symmetry-breaking groups X by virtue of (i) their influence on the energy profile for rotation about the ester C−O bond, (ii) their contribution to the core transverse dipole moment, and (iii) their influence on core−core interactions with surrounding SmC host molecules. To investigate these relationships, we have synthesized a series of four new dopants, **2**−**5**, with core structures analo-

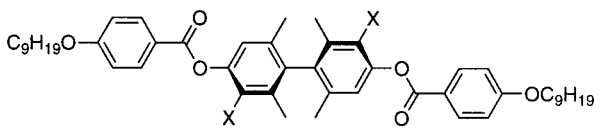

1, X=NO_2; **2**, X=F; **3**, X=Cl; **4**, X=Br; **5**, X=CH_3

(5) Kuczynski, W.; Stegemeyer, H. *Chem. Phys. Lett.* **1980**, *70*, 123.
(6) Stegemeyer, H.; Meister, R.; Hoffmann, U.; Sprick, A.; Becker, A. *J. Mater. Chem.* **1995**, *5*, 2183.
(7) Osipov, M. A.; Stegemeyer, H.; Sprick, A. *Phys. Rev. E* **1996**, *54*, 6387.
(8) Vizitiu, D.; Lazar, C.; Halden, B. J.; Lemieux, R. P. *J. Am. Chem. Soc.* **1999**, *121*, 8229.

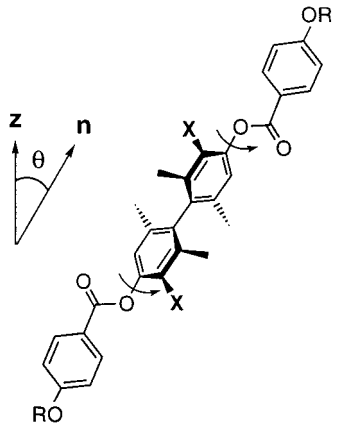

Figure 3. Rotation of the atropisomeric core about the two ester C−O bonds in the SmC* phase. The vectors **z** and **n** are in the plane of the page and the polar axis is normal to the plane of the page.

Scheme 1[a]

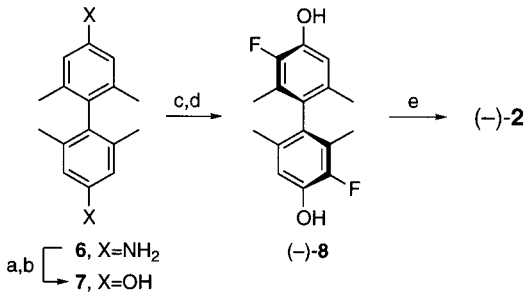

[a] (a) $NaNO_2$, concentrated H_2SO_4, 0 °C; (b) 20% aqueous H_2SO_4, △; (c) PyF^+ OTf^-, $C_2H_2Cl_4$, 100 °C; (d) CSP HPLC resolution, Daicel Chiralcel OJ column, 95:5 hexanes/EtOH, 4 mL/min; (e) 4-nonyloxybenzoyl chloride, DMAP, THF, △.

gous to **1**, but with different symmetry-breaking groups X, and measured their polarization powers in the four SmC hosts previously used in the study of dopant **1** (Figure 2).[10]

Results

Synthesis. The dopants **2**−**5** are new compounds that were synthesized in optically pure (>99% ee for **3**−**5**) or near optically pure form (93% ee for **2**). The diol precursor to dopant (−)-**2** was obtained by treatment of the known diol **7** with *N*-fluoropyridinium triflate (Scheme 1). Resolution of (±)-**8** was achieved by chiral-phase HPLC on a Daicel Chiralcel OJ semi-prep column and was followed by esterification. The diol precursor to dopant (−)-**5** is a known compound[11] that was resolved by chiral-phase HPLC on a Daicel Chiralpak AS semi-prep column and then esterified. The diol precursor to dopant (+)-**3** were obtained by chlorination of the known benzidine **6**[12] with *N*-chlorosuccinimide

Scheme 2[a]

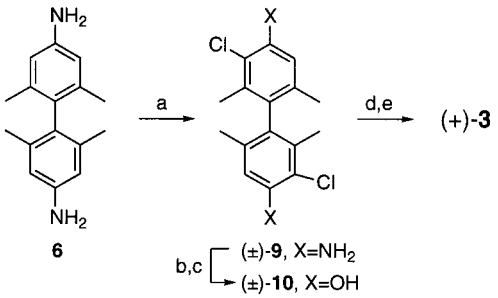

[a] (a) NCS, CH_3CN, 60 °C; (b) $NaNO_2$, concentrated H_2SO_4, 0 °C; (c) 20% aqueous H_2SO_4, △; (d) 4-nonyloxybenzoyl chloride, DMAP, THF, △; (e) CSP HPLC resolution, Regis (*S*,*S*)-Whelk-O1 column, 91.5:8.5 hexanes/dichloroethane, 5 mL/min.

followed by hydrolysis of the corresponding bis-diazonium salt (Scheme 2). Similarly, the diol precursor to dopant (+)-**4** was obtained by bromination of the diacetamide derivative of **6** followed by hydrolysis of the corresponding bis-diazonium salt. After esterification, the racemic diesters (±)-**3** and (±)-**4** were resolved by chiral-phase HPLC on a Regis (*S*,*S*)-Whelk-O1 semi-prep column. All optically active dopants were carefully recrystallized from either hexanes or absolute EtOH to remove ionic impurities prior to doping in SmC liquid crystal hosts.

Ferroelectric Polarization and Helical Pitch Measurements. The dopants **2**−**5** were mixed into the SmC hosts **PhB**, **NCB76**, **DFT**, and **PhP1** over the mole fraction range $0.01 < x_d \leq 0.05$ to produce a chiral SmC* phase.[13] Alignment of the SmC* mixtures in polyimide-coated ITO glass cells with a 4-μm spacing produced SSFLC films suitable for measurement of ferroelectric properties. Spontaneous polarizations P_S and tilt angles θ were measured at 5 K below the SmC*−SmA* phase transition temperature ($T - T_C = -5$ K) by the triangular wave method[14] and the corresponding P_o values derived according to eq 2. Plots of P_o versus x_d gave good linear fits ($R^2 = 0.960-0.998$) except in the case of **4** in **PhP1**, which gave a nonlinear plot that was fitted to an exponential function ($R^2 = 0.984$). Polarization power values were derived from the corresponding fits according to eq 1. As shown in Table 1, the dopants **2**−**4** gave a measurable spontaneous polarization in all SmC hosts except **PhB** up to $x_d = 0.05$. The hexamethyl dopant **5** gave a measurable spontaneous polarization in **PhP1** only. Upper limits for δ_p were estimated based on the instrument detection limit (0.3 nC/cm^2) and the observed tilt angle at $T - T_C = -5$ K. To study the relationship between δ_p and chirality transfer, the helical pitch p of SmC* phases induced by **2**−**5** in **NCB76** and **PhP1** were measured by polarized light microscopy at a constant dopant mole fraction, $x_d = 0.02$ (Table 1). The helical structure of the SmC* phase is a macroscopic manifestation of chiral induction, and the inverse pitch $1/p$ is taken as a measure of intermolecular chirality transfer.

Conformational Analyses. To model the effect of varying the symmetry-breaking groups X on the rota-

(9) A similar chirality transfer mechanism was proposed for cholesteric liquid crystal phases induced by atropisomeric dopants: (a) Gottarelli, G.; Hibert, M.; Samori, B.; Solladié, G.; Spada, G. P.; Zimmermann, R. *J. Am. Chem. Soc.* **1983**, *105*, 7318. (b) Spada, G. P.; Proni, G. *Enantiomer* **1999**, *3*, 301.

(10) A preliminary account of this work was presented at the 6th International Conference on Ferroelectric Liquid Crystals, Brest, France, 1997: Vizitiu, D.; Halden, B. J.; Lemieux, R. P. *Ferroelectrics* **1998**, *212*, 257.

(11) Tanaka, K.; Moriyama, A.; Toda, F. *J. Chem. Soc., Perkin Trans. 1* **1996**, 603.

(12) Carlin, R. B. *J. Am. Chem. Soc.* **1945**, *67*, 928.

(13) Doping compounds **2**−**5** into any of the SmC hosts caused the temperature range of the SmC* phase to decrease with increasing x_d, thus limiting the useful range to $x_d \leq 0.05$.

(14) Miyasato, K.; Abe, S.; Takezoe, H.; Fukuda, A.; Kuze, E. *Jpn. J. Appl. Phys.* **1983**, *22*, L661.

Table 1. Polarization Power δ_p of Dopants 1−5 and Helical Pitch p of the SmC* Phases Induced in the Liquid Crystal Hosts PhB, DFT, NCB76, and PhP1

			δ_p (nC/cm^2)[a,b]				p (μm)[g,h]	
dopant	X	$\langle\mu_\perp\rangle$ (D)[c]	**PhB**	**DFT**	**NCB76**	**PhP1**	**NCB76**	**PhP1**
(−)-1	NO_2	3.34	<34 (−)[d,e]	312 ± 32 (−)[d]	514 ± 38 (−)[d]	1555 ± 119 (−)[d]	5.9 ± 0.6[d]	2.9 ± 0.3[d]
(−)-2	F	0.580	<40 (+)[e,f]	59 ± 6 (+)[f]	94 ± 3 (+)[f]	255 ± 36 (+)[f]	14.0 ± 1.5[f]	4.2 ± 0.6[f]
(+)-3	Cl	0.627	<30 (+)[e]	60 ± 7 (+)	116 ± 7 (+)	197 ± 28 (+)	18.3 ± 1.9	4.3 ± 0.5
(+)-4	Br	0.262	<20 (+)[e]	42 ± 1 (+)	83 ± 4 (+)	34 (+)	24.9 ± 2.5	24.8 ± 4.5
(−)-5	CH_3	−0.654	<26 (−)[e]	<60 (−)[e]	<43 (−)[e]	46 ± 6 (−)	>40	36.3 ± 5.6

[a] Sign of induced P_S in parentheses. [b]Uncertainty is ± standard error of least-squares fit. [c]Statistical average transverse dipole moment of the core/diester unit at 346 K. [d]From ref 8. [e]Estimated upper limit based on a detection limit of 0.3 nC/cm^2 at the highest dopant mole fraction. [f] Values normalized to dopant optical purity of 100% ee. [g]Measured at a dopant mole fraction $x_d = 0.02$. [h] Uncertainty is ±1 standard deviation.

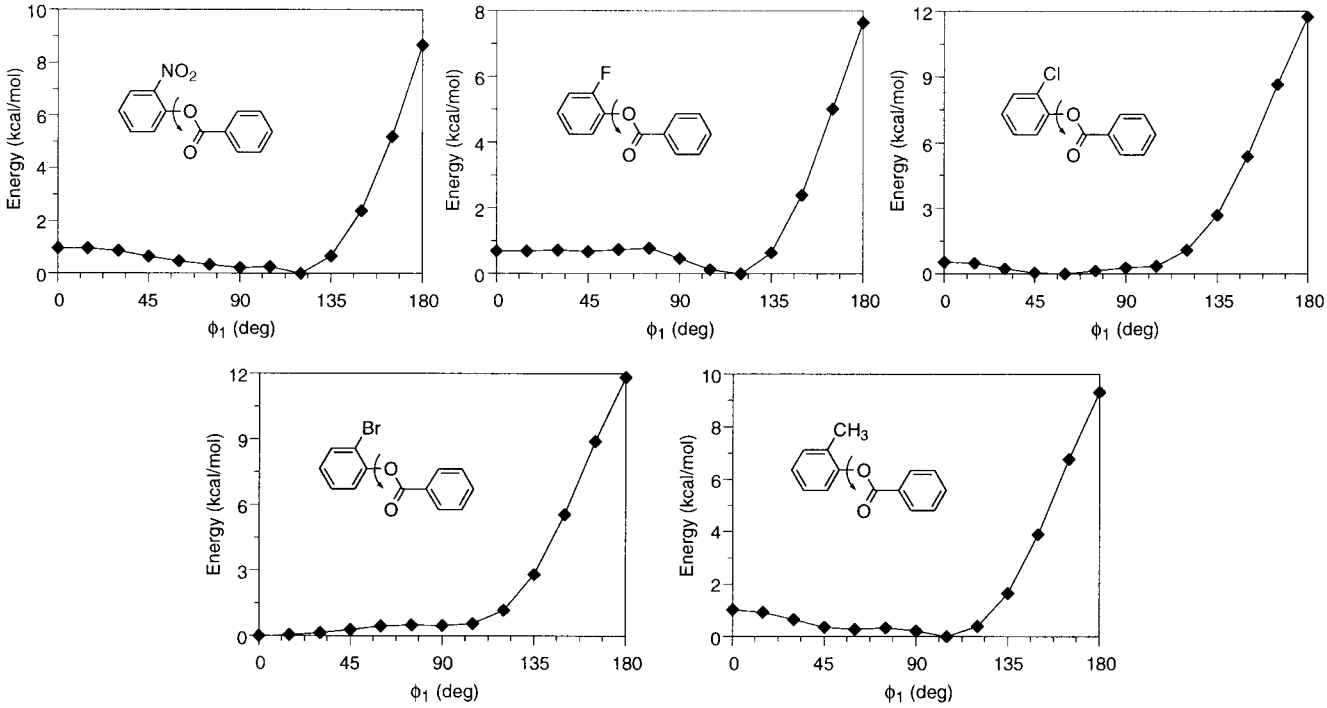

Figure 4. Energy profiles for a series of 2-substituted phenyl benzoates (**11a**) as a function of the torsional angle defined by atoms 1, 2, 3, and 4 according to B3LYP/6-31G(d) calculations.

tional asymmetry of the atropisomeric cores, energy profiles for rotation about the ester C−O bond in substructures **11a** (half-core) were calculated as a function of the dihedral angle defined by atoms 1−2−3−4 (ϕ_1) at 15° intervals over the range $0° \le \phi_1 \le 180°$.[15] For each conformation, the dihedral angle ϕ_1 was constrained at its predetermined value and the dihedral angle defined by atoms 3−4−5−6 (ϕ_2) was fixed at 0°.[16] The structure was then optimized using the RHF/6-31G-(d) method,[17] followed by single-point energy and dipole moment calculations using Becke's three-parameter hybrid density functional with the Lee, Yang, and Parr correlation functional (B3LYP)[18] and the 6-31G(d) basis set. The resulting rotational energy profiles shown in Figure 4 suggest that the energy surface for rotation of

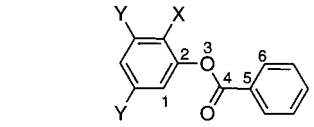

11a, Y=H
11b, Y=CH_3

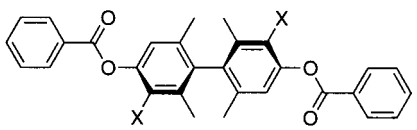

12, X=NO_2, F, Cl, Br, CH_3

(15) Preliminary conformational analysis and dipole moment calculations on the full half-core structure **11b** gave similar results to those obtained with the abbreviated half-core structure **11a**.

(16) Deviations from a dihedral angle ϕ_2 of 0° are energetically unfavorable and can produce diastereomeric configurations that unnecessarily complicate the calculations. Variation in ϕ_2 has been shown to have little effect on the overall dipole moment of the conformation.

(17) Frisch, M. J.; Trucks, G. W.; Schlegel, H. B.; Scuseria, G. E.; Robb, M. A.; Cheeseman, J. R.; Zakrzewski, V. G.; Montgomery, J. A., Jr.; Stratmann, R. E.; Burant, J. C.; Dapprich, S.; Millam, J. M.; Daniels, A. D.; Kudin, K. N.; Strain, M. C.; Farkas, O.; Tomasi, J.; Barone, V.; Cossi, M.; Cammi, R.; Mennucci, B.; Pomelli, C.; Adamo, C.; Clifford, S.; Ochterski, J.; Petersson, G. A.; Ayala, P. Y.; Cui, Q.; Morokuma, K.; Malick, D. K.; Rabuck, A. D.; Raghavachari, K.; Foresman, J. B.; Cioslowski, J.; Ortiz, J. V.; Stefanov, B. B.; Liu, G.; Liashenko, A.; Piskorz, P.; Komaromi, I.; Gomperts, R.; Martin, R. L.; Fox, D. J.; Keith, T.; Al-Laham, M. A.; Peng, C. Y.; Nanayakkara, A.; Gonzalez, C.; Challacombe, M.; Gill, P. M. W.; Johnson, B. G.; Chen, W.; Wong, M. W.; Andres, J. L.; Head-Gordon, M.; Replogle, E. S.; Pople, J. A. *Gaussian 98*, revision A.7; Gaussian, Inc.: Pittsburgh, PA, 1998.

(18) Becke, A. D. *J. Chem. Phys.* **1993**, *98*, 1372.

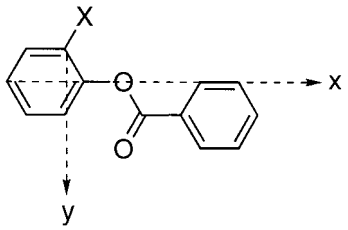

Figure 5. Frame of reference used in the calculations of transverse dipole moments. The *x* and *y* axes are in the plane of the page.

the core about the C−O bond of the ester group is relatively flat in the range $0° \le \phi_1 \le 120°$. Interestingly, the profiles calculated for 2-fluoro and 2-nitrophenyl benzoate give global minima at $\phi_1 = 120°$ with the carbonyl group syn to the X group, which is counterintuitive on both steric and electrostatic grounds, and at variance with previous calculations using the semiempirical AM1 method.[8,10] Similar results were obtained with RHF and MP2 methods using the same basis set. In the halide series, the increasing steric demand of the X group appears to override this effect as the global minimum shifts from $\phi_1 = 120°$ for 2-fluorophenyl benzoate to $\phi_1 = 0°$ for 2-bromophenyl benzoate.

Calculation of Transverse Dipole Moments. To study the influence of the symmetry-breaking groups X on the polar ordering of dopants **1**−**5** in the four SmC hosts, the polarization power values were normalized for differences in transverse dipole moments of the atropisomeric cores. Because of steric coupling of the polar ester groups to the rigid biphenyl core, transverse dipole moments were calculated as Boltzmann-weighted statistical averages over all possible conformations of the core/diester units **12** based on the rotational energy profiles calculated for substructures **11a**.

The transverse dipole moments were calculated using a molecule-fixed orthonormal reference frame for each optimized conformation, with the direction of the *x* and *y* axes defined as shown in Figure 5, and the *z* axis taken as the cross product of the normalized *x* and *y* axes. The dipole moment for each conformation was transformed to this reference frame to give components along the *x*, *y*, and *z* axes (μ_x, μ_y, and μ_z). Boltzmann-weighted statistical average dipole moments along the *y* axis ($\langle\mu_y\rangle$) were calculated at a temperature of 346 K (corresponding to the average temperature at which the P_s measurements were taken in **DFT**, **NCB76**, and **PhP1**) from

$$\langle\mu_y\rangle = \int_0^{2\pi}\mu_y(\phi_1)\exp[-E(\phi_1)/k_BT]\,d\phi_1 \Big/ \int_0^{2\pi}\exp[-E(\phi_1)/k_BT]\,d\phi_1 \quad (3)$$

where k_B is Boltzmann's constant and *T* is the absolute temperature. Contributions of the *z* components of the dipole moment to the statistical average were ignored because, for each of the minimized conformers with $0° \le \phi_1 \le 180°$, there exists an enantiomeric structure with $\phi_1 = -\phi_1$ whose *z* component of the dipole moment is equal but opposite. Likewise, when the two half-cores are put together to give the transverse dipole of the full core/diester unit ($\langle\mu_\perp\rangle$), the *x* components of the two dipole moments in any conformation are equal but opposite. In the full core, the biphenyl group is treated as conformationally rigid, with the dihedral angle formed by the two phenyl rings fixed at 90°, so the total statistical average transverse dipole moment $\langle\mu_\perp\rangle$ is simply given by $\langle\mu_\perp\rangle = 2\langle\mu_y\rangle \sin(\pi/4)$. The resulting $\langle\mu_\perp\rangle$ values (in Debye) are listed in Table 1, and normalized polarization power values $\delta_{p(norm)}$ are obtained by dividing δ_p by the corresponding $\langle\mu_\perp\rangle$ values.

Discussion

As previously observed for dopant **1**,[8] the polarization power of dopants **2**−**5** strongly depends on the nature of the SmC host, with δ_p increasing in the order **PhB** ≪ **DFT** < **NCB76** < **PhP1**. Furthermore, in a given SmC host, δ_p varies with the nature of the symmetry-breaking groups X, which is due in part to the corresponding variation in the transverse dipole moment of the core. By using Boltzmann-weighted statistical average transverse dipole moments to calculate $\delta_{p(norm)}$ values, differences in rotational asymmetry of the atropisomeric core in the absence of intermolecular interactions are included in the normalization. Hence, an analysis of $\delta_{p(norm)}$ values can provide useful information on the effect of core−core interactions between dopant and SmC host molecules on polar ordering of the atropisomeric dopants within the frameworks of current models for Type II host effects (vide infra).

The Boulder Model. The orientational and conformational ordering of a chiral dopant in a SmC phase is modeled by a mean-field potential that qualitatively behaves like a binding site analogous to that described in organic host−guest chemistry and biochemistry.[3,19,20] The Boulder model assumes that the SmC mean field potential has a zigzag form[21] so that the molecular side chains are, on average, less tilted with respect to the smectic layer normal **z** than is the molecular core. Within the confines of this achiral binding site, the orientational distribution of a molecule around its long axis acquires polar character (i.e., molecular orientations related by a 180° rotation about the molecular long axis **n** are no longer energetically equivalent). For a chiral dopant molecule, steric coupling of a polar functional group to an adjacent chiral center causes a desymmetrization of the functional group's conformational energy profile. This conformational asymmetry, in combination with the polar orientational ordering imposed by the binding site, results in an orientational bias of the dipole moment along the polar C_2 axis.

Recent simulations have shown that large variations in P_S can be achieved for a given Type II dopant by simply varying the length of the core section of the achiral zigzag binding site.[22] This suggests that the polar ordering of dopants with chiral cores may simply be a function of the thickness of the SmC core sublayer, which is defined by the host structure and is independent of core−core interactions. On the other hand, it is possible that core−core interactions between chiral dopant and surrounding host molecules cause an achiral

(19) Glaser, M. A.; Ginzburg, V. V.; Clark, N. A.; Garcia, E.; Walba, D. M.; Malzbender, R. *Mol. Phys. Rep.* **1995**, *10*, 26.

(20) Glaser, M. A. In *Advances in the Computer Simulations of Liquid Crystals*; Zannoni, C., Pasini, P., Eds.; Kluwer: Dordrecht, 1999; pp 263−331.

(21) The zigzag model for the SmC phase was originally proposed by: Bartolino, R.; Doucet, J.; Durand, G. *Ann. Phys.* **1978**, *3*, 389.

(22) Nendel, M.; Glaser, M. A., unpublished results.

distortion of the simple zigzag binding site that results in a change in the orientational distribution of the dopant transverse dipole moment with respect to the polar axis. This *biaxial ordering* model is consistent with one of the microscopic models proposed by Stegemeyer to explain the Type II host effect[6,7] and with the Boulder model's basic assumption that the binding site maintains reflection symmetry.

The Chirality Transfer Feedback Model. In another microscopic model, Stegemeyer suggested that core−core interactions may contribute to the Type II host effect by causing the polar ordering of nearby SmC host molecules through intermolecular chirality transfer (i.e., both dopant and nearby host molecules contribute to P_S, especially when the SmC host has a large transverse dipole moment). To explain the remarkably high polarization power of dopant **1** in the phenylpyrimidine host **PhP1**, which has virtually no transverse dipole moment, we proposed that chirality transfer to surrounding SmC host molecules causes a *chiral distortion* of the zigzag binding site.[8] As a feedback, the chiral distortion amplifies δ_p by increasing the rotational asymmetry of the atropisomeric core with respect to the dopant side chains by virtue of diastereomeric relationships between the various chiral rotamers of the dopant and the chiral binding site. Recently, we obtained the first experimental evidence of a chiral distortion of the binding site in **PhP1** by studying the effect of dopant **1** on the spontaneous polarization induced by a probe phenylpyridine dopant with a chiral 2,3-difluorooctyloxy side chain, which mimics the phenylpyrimidine SmC host.[23,24]

Analysis of $\delta_{p(norm)}$ as a Function of X. Variations in $\delta_{p(norm)}$ as a function of the SmC host and as a function of X may be rationalized by considering the relative contributions of achiral and chiral distortions of the zigzag binding site. According to the Boulder model, the results obtained in the SmC host **PhB** may be attributed to a binding site shape that forces the transverse dipole of the atropisomeric core $\langle\mu_\perp\rangle$ to lie near the tilt plane of the SmC* phase. The higher $\delta_{p(norm)}$ values obtained in **DFT**, **NCB76**, and **PhP1** may then be attributed to achiral distortions of the binding site that cause a shift in the orientational distribution of $\langle\mu_\perp\rangle$ toward the polar axis. However, the unique profile of the $\delta_{p(norm)}$ vs X bar graph in **PhP1** (Figure 6) suggests that another host effect, which we attribute to the chirality transfer feedback (CTF) mechanism (vide infra), makes significant contribution to polar ordering in **PhP1**.

The similar profiles of the $\delta_{p(norm)}$ vs X bar graphs in **DFT** and **NCB76** are more consistent with the Boulder model. The approximate invariance of $\delta_{p(norm)}$ vs X for dopants **1**−**3** in **DFT** and **NCB76** suggests that the core transverse dipoles have approximately the same orientational distribution with respect to the polar axis. In the case of dopant **4**, the higher $\delta_{p(norm)}$ values may be attributed to a change in orientational distribution of $\langle\mu_\perp\rangle$ due to the higher steric demand of the bromo substituents. The lack of correlation between $\delta_{p(norm)}$ and the inverse SmC* pitch $1/p$ in **NCB76** (Figure 7) suggests that intermolecular chirality transfer does not influence polar ordering significantly, although one might argue that the remarkably small $\delta_{p(norm)}$ estimated for dopant **5**—a compound very similar to **3** in terms of steric demand, polarizability, and transverse dipole moment, but which induces a much longer SmC* pitch in **NCB76**—is due in large part to its inability to desymmetrize the binding site. In **PhP1**, $\delta_{p(norm)}$ vs X clearly follows a different trend, and $\delta_{p(norm)}$ correlates with the inverse SmC* pitch (Figure 7), which suggests that chirality transfer contributes significantly to polar ordering of the atropisomeric dopants according to the CTF model. This is consistent with the favorable structural match of dopant and SmC host core structures for chirality transfer via core−core interactions and with similar correlations found in a previous study.[8]

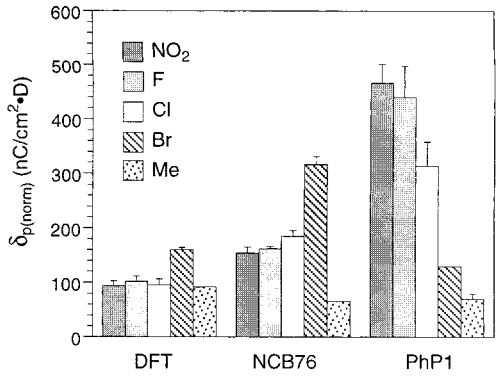

Figure 6. Normalized polarization power $\delta_{p(norm)}$ for dopants **1**−**5** in the SmC hosts **DFT**, **NCB76**, and **PhP1**. The $\delta_{p(norm)}$ values for dopant **5** (X = Me) in **DFT** and **NCB76** are estimated upper limits. Error bars represent +SE.

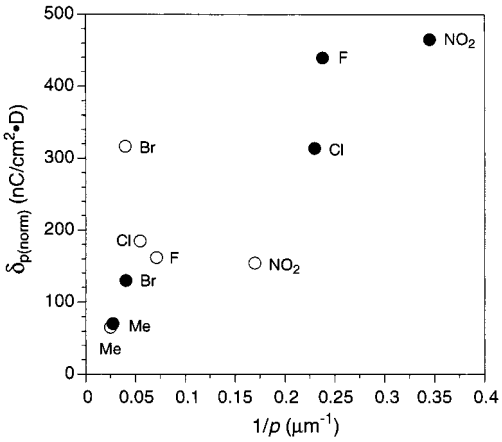

Figure 7. Normalized polarization power $\delta_{p(norm)}$ as a function of inverse SmC* pitch $1/p$ in the SmC hosts **PhP1** (filled circles) and **NCB76** (open circles). The $1/p$ value for X = Me in **NCB76** is an upper limit estimate.

Summary

Four new chiral dopants (**2**−**5**) containing an atropisomeric biphenyl core derived from 4,4′-dihydroxy-2,2′,6,6′-tetramethylbiphenyl with different symmetry-breaking groups at the 3,3′-positions (X = F, Cl, Br, and Me) were synthesized in an optically active form. The polarization powers δ_p of these dopants were measured in four SmC liquid crystal hosts with different core

(23) Lazar, C.; Wand, M. D.; Lemieux, R. P. *J. Am. Chem. Soc.* **2000**, *122*, 12586.

(24) The observation of cooperative effects in P_o vs x_d plots, which would be consistent with a chiral distortion of the binding site and the CTF model, is precluded by the dopant mole fraction limit of 0.05 (see footnote 13).

structures and compared to δ_p values previously obtained for the corresponding dopant **1** with X = NO_2. As previously observed for dopant **1**, the polarization power of dopants **2**−**5** depends on the nature of the SmC host, with δ_p increasing in the order **PhB** ≪ **DFT** < **NCB76** < **PhP1**, and on the nature of the symmetry-breaking groups X. Theoretical conformational analyses for rotation of the atropisomeric cores about the ester C−O bonds were performed at the B3LYP/6-31G(d) level and used in calculating Boltzmann-weighted statistical average transverse dipole moments $\langle\mu_\perp\rangle$ of the core−diester units. The $\langle\mu_\perp\rangle$ values were used to normalize δ_p to study the influence of groups X on polar ordering of the dopants. Variations in $\delta_{p(norm)}$ are rationalized using models describing either achiral or chiral distortions of the zigzag binding site of the SmC host. Results show that the symmetry-breaking groups X exert a unique influence on polar ordering of the dopants in the phenylpyrimidine host **PhP1** that is consistent with a model in which chirality transfer via core−core interactions between dopant and host molecules causes a chiral distortion of the zigzag binding site.

Experimental Section

General. ^{1}H and ^{13}C NMR spectra were recorded on Bruker ACF-200 and AM-400 NMR spectrometers in deuterated chloroform ($CDCl_3$) and deuterated dimethyl sulfoxide (DMSO-d_6). The chemical shifts are reported in δ (ppm) relative to tetramethylsilane as the internal standard. Low-resolution EI mass spectra were recorded on a Fisons VG Quattro triple quadrupole mass spectrometer; peaks are reported as *m*/*z* (% intensity relative to the base peak). High-resolution EI mass spectra were performed by the University of Ottawa Regional Mass Spectrometry Center. Optical rotations were measured on a Perkin−Elmer 241 polarimeter at room temperature. Semipreparative chiral stationary phase HPLC separations were performed using 25 cm × 10 mm i.d. Regis (*S*,*S*)-Whelk-O1, Daicel Chiralcel OJ and Chiralpak AS columns. Elemental analyses were performed by Guelph Chemical Laboratories Ltd. (Guelph, Ontario) and by MHW Laboratories (Phoenix, AZ). Melting points were measured on a Mel-Temp II melting point apparatus and are uncorrected.

Materials. All reagents, chemicals, and liquid crystal hosts were obtained from commercial sources and used without further purification unless otherwise noted. Methylene chloride (CH_2Cl_2) was distilled from P_2O_5 under N_2. Tetrahydrofuran (THF) was distilled from sodium/benzophenone under N_2. (−)-2,2′,6,6′-Tetramethyl-3,3′-dinitro-4,4′-bis[(4-nonyloxybenzoyl)-oxy]biphenyl (**(−)-1**),[8] 4,4′-diamino-2,2′,6,6′-tetramethylbiphenyl (**6**),[12] 4,4′-dihydroxy-2,2′,6,6′-tetramethylbiphenyl (**7**),[8] (±)-4,4′-dihydroxy-2,2′,3,3′,6,6′-hexamethylbiphenyl (**(±)-16**),[11] (±)-4-[(4-methylhexyl)oxy]phenyl 4-decyloxybenzoate (**PhB**),[25] and 2′,3′-difluoro-4-heptyl-4″-nonyl-*p*-terphenyl (**DFT**)[26] were synthesized according to published procedures and shown to have the expected physical and spectral properties. The liquid crystal host **NCB76** was provided by Prof. H. Stegemeyer.

(−)-3,3′-Difluoro-4,4′-dihydroxy-2,2′,6,6′-tetramethylbiphenyl ((−)-8). Under an Ar atmosphere, 0.404 g of *N*-fluoropyridinium triflate (1.64 mmol) was added to a solution of **7** (0.198 g, 0.82 mmol) in 1,1,2,2-tetrachloroethane (3 mL) and the mixture was stirred at 100 °C for 24 h. After cooling, the mixture was diluted with Et_2O (20 mL), washed with water, dried ($MgSO_4$), and concentrated. Purification by flash chromatography on silica gel (7:3 hexanes/EtOAc) gave 81 mg (38%) of **(±)-8** as a white-yellow solid. The product was resolved by chiral-phase HPLC using a Daicel Chiralcel OJ column (95:5 hexanes/EtOH, 4 mL/min). The first eluant was collected and concentrated to give **(−)-8** with an optical purity of 93% ee: mp 75−76 °C; $[\alpha]_D^{25}$ −5.7 (*c* 0.1, $CHCl_3$); ^{1}H NMR (200 MHz, $CDCl_3$) δ 1.81 (s, 6H), 1.82 (s, 6H), 5.09 (s, 2H), 6.78 (d, J = 8.8 Hz, 2H); ^{13}C NMR (100 MHz, $CDCl_3$) δ 11.5, 19.4, 115.5, 123.6 (d, J = 13.1 Hz), 131.4, 132.1, 142.0 (d, J = 15.1 Hz), 148.3 (d, J = 231.6 Hz); MS (EI) *m*/*z* 278 (M+, 100), 248 (24), 243 (32), 215 (16); HRMS (EI) calcd for $C_{16}H_{16}F_2O_2$: 278.1118. Found: 278.1105.

(−)-3,3′-Difluoro-2,2′,6,6′-tetramethyl-4,4′-bis[(4-*n*-nonyloxybenzoyl)oxy]biphenyl ((−)-2). Under an Ar atmosphere, solid DCC (25 mg, 0.12 mmol) was added to a stirred solution of **(−)-8** (17 mg, 0.06 mmol), 4-nonyloxybenzoic acid (32 mg, 0.12 mmol), and DMAP (15 mg, 0.12 mmol) in dry CH_2Cl_2 (5 mL). The mixture was stirred at room temperature for 24 h, then filtered, and concentrated. The solid residue was redissolved in EtOAc and washed with 2 M aq HCl, water, and brine, then dried ($MgSO_4$), and concentrated. Purification by flash chromatography on silica gel (7:3 hexanes/EtOAc) gave 22 mg (46%) of (−)-**2** as a white solid. The compound was further purified by recrystallization from absolute EtOH after filtration through a 0.45-μm PTFE filter: mp 128−130 °C; ^{1}H NMR (400 MHz, $CDCl_3$) δ 0.89 (t, J = 6.7 Hz, 6H), 1.26−1.50 (m, 24H), 1.79−1.87 (m, 4H), 1.90 (s, 6H), 1.91 (s, 6H), 4.05 (t, J = 6.5 Hz, 4H), 6.99 (d, J = 8.8 Hz, 4H), 7.05 (d, J = 7.4 Hz, 2H), 8.17 (d, J = 8.8 Hz, 4H); ^{13}C NMR (100 MHz, $CDCl_3$) δ 11.8, 14.1, 19.3, 22.6, 25.9, 29.1, 29.2, 29.3, 29.5, 29.7, 31.8, 68.3, 114.3, 120.8, 122.3, 124.4 (d, J = 13.7 Hz), 131.5, 132.4, 137.2 (d, J = 13 Hz), 151.3 (d, J = 243.8 Hz), 163.6, 164.1. Anal. Calcd for $C_{48}H_{60}F_2O_6$: C, 74.78; H, 7.84; F, 4.93. Found: C, 74.79; H, 7.72; F, 5.19.

(±)-4,4′-Diamino-3,3′-dichloro-2,2′,6,6′-tetramethylbiphenyl ((±)-9). To a solution of **6** (0.27 g, 1.13 mmol) in acetonitrile (4 mL) heated to 60 °C was added 0.30 g (2.25 mmol) of solid *N*-chlorosuccinimide. The mixture was refluxed overnight with stirring, then cooled, and concentrated. The residue was redissolved in EtOAc and washed twice with 5% aqueous NaOH, dried ($MgSO_4$), and concentrated. Purification by flash chromatography on silica gel (4:1 hexanes/EtOAc) gave 0.26 g (75%) of **(±)-9** as a beige solid: mp 135−136 °C; ^{1}H NMR (400 MHz, $CDCl_3$) δ 1.77 (s, 6H), 1.92 (s, 6H), 3.97 (s, 4H), 6.59 (s, 2H); ^{13}C NMR (100 MHz, $CDCl_3$) δ 17.3, 19.9, 114.7, 117.7, 131.1, 134.6, 135.2, 141.4; MS (EI) *m*/*z* 312 (M + 4, 11), 310 (M + 2, 66), 308 (M+, 100), 258 (48), 129 (36), 111 (47); HRMS (EI) calcd for $C_{16}H_{18}Cl_2N_2$: 308.0847. Found: 308.0842.

(±)-3,3′-Dichloro-4,4′-dihydroxy-2,2′,6,6′-tetramethylbiphenyl ((±)-10). A solution of $NaNO_2$ (0.14 g, 2.0 mmol) in water (4 mL) was added dropwise to a solution of **(±)-9** (0.28 g, 0.91 mmol) in 10% aqueous H_2SO_4 (20 mL) cooled to 5 °C. The mixture was stirred at 5 °C for 45 min and then filtered. The resulting solution was diluted with 20% aqueous H_2SO_4 (10 mL), refluxed for 3 h, then cooled, and extracted with EtOAc (2 × 20 mL). The combined extracts were washed with water and brine, dried ($MgSO_4$), and concentrated. Purification by flash chromatography on silica gel (7:3 hexanes/EtOAc) gave 0.23 g (80%) of **(±)-10** as an orange solid: mp 110−111 °C; ^{1}H NMR (400 MHz, $CDCl_3$) δ 1.82 (s, 6H), 1.94 (s, 6H), 5.59 (s, 2H), 6.85 (s, 2H); ^{13}C NMR (100 MHz, $CDCl_3$) δ 17.2, 19.9, 114.8, 118.2, 132.6, 134.4, 136.1, 150.1; MS (EI) *m*/*z* 314 (M + 4, 11), 312 (M + 2, 66), 310 (M+, 100), 260 (100), 240 (57), 225 (56), 82 (63); HRMS (EI) calcd for $C_{16}H_{16}Cl_2O_2$: 310.0527. Found: 310.0547.

(+)-3,3′-Dichloro-2,2′,6,6′-tetramethyl-4,4′- bis[(4-*n*-nonyloxybenzoyl)oxy]biphenyl ((+)-3). The procedure described for the synthesis of **(−)-2** was followed using **(±)-10** (0.21 g, 0.66 mmol) to give 0.38 g (70%) of **(±)-3** as a white solid. The product was resolved by chiral-phase HPLC using a Regis (*S*,*S*)-Whelk-O1 column (91.5:8.5 hexanes/dichloroethane, 5 mL/min). The first eluant was collected and concentrated and the residue recrystallized from absolute EtOH after filtration through a 0.45-μm PTFE filter to give **(+)-3** in optically pure form: mp 128−130 °C; $[\alpha]_D^{24}$ +10.0 (c 0.24 $CHCl_3$); ^{1}H NMR (400 MHz, $CDCl_3$) δ 0.89 (t, J = 6.9 Hz, 6H),

(25) Keller, P. *Ferroelectrics* **1984**, *58*, 3.
(26) Gray, G. W.; Hird, M.; Lacey, D.; Toyne, K. J. *J. Chem. Soc., Perkin Trans. 2* **1989**, 2041.

1.23−1.50 (m, 24H), 1.80−1.86 (m, 4H), 1.92 (s, 6H), 2.04 (s, 6H), 4.05 (t, J = 6.5 Hz, 4H), 6.99 (d, J = 8.9 Hz, 4H), 7.12 (s, 2H), 8.20 (d, J = 8.9 Hz, 4H); ^{13}C NMR (100 MHz, $CDCl_3$) δ 14.1, 17.3, 19.8, 22.6, 25.9, 29.0, 29.2, 29.3, 29.5, 31.8, 68.3, 114.3, 121.0, 122.6, 125.2, 132.4, 135.1, 135.5, 137.8, 146.4, 163.6, 164.1. Anal. Calcd for $C_{48}H_{60}Cl_2O_6$: C, 71.72; H, 7.52; Cl, 8.82. Found: C, 71.68; H, 7.67; Cl, 8.68.

(±)-4,4′-Diacetamido-3,3′-dibromo-2,2′,6,6′-tetramethylbiphenyl ((±)-13). A solution of **6** (1.0 g, 4.16 mmol) in acetic anhydride (3 mL) was stirred for 5 h at room temperature and then poured over ice/water (500 mL). The pink precipitate was collected by filtration, washed with H_2O, and dried in a vacuum oven to give 1.23 g of 4,4′-diacetamido-2,2′,6,6′-tetramethylbiphenyl. The crude product was dissolved in boiling glacial acetic acid (5 mL) and then cooled to 5 °C and neat Br_2 (0.4 mL, 7.6 mmol) was added dropwise to the solution. The mixture was stirred at 50 °C for 24 h and then poured over ice/water (200 mL) containing sodium metabisulfite. The resulting precipitate was filtered, washed with water, and dried in a vacuum oven. Purification by flash chromatography on silica gel (95:5 $CHCl_3$/CH_3OH) gave 1.65 g (90%) of **(±)-13** as a white solid: mp 235−237 °C; ^{1}H NMR (200 MHz, $CDCl_3$) δ 1.86 (s, 6H), 2.01 (s, 6H), 2.26 (s, 6H), 7.73 (s, 2H), 8.17 (s, 2H); ^{13}C NMR (50 MHz, $CDCl_3$) δ 20.1, 20.8, 24.9, 114.1, 120.8, 134.7, 135.7, 135.9, 136.5, 168.2; MS (EI) m/z 484 (M + 4, 4), 482 (M + 2, 7), 480 (M+, 4), 404 (13), 403 (57), 401 (58), 361 (16), 359 (16), 167 (32), 149 (100), 120 (26), 119 (17), 118 (26), 117 (16).

(±)-4,4′-Diamino-3,3′-dibromo-2,2′,6,6′-tetramethylbiphenyl ((±)-14) A solution of **(±)-13** (0.642 g, 1.33 mmol) in absolute EtOH (6 mL) and concentrated HCl (1 mL) was refluxed overnight with stirring. After cooling, the mixture was diluted with water (10 mL) and the EtOH was removed in vacuo. The residue was poured into ice/water (150 mL) and neutralized with 5% aqueous NaOH. The resulting precipitate was filtered, washed with water, and dried in a vacuum oven to give 0.51 g (96%) of **(±)-14** as a white solid: mp 156−158 °C; ^{1}H NMR (200 MHz, $CDCl_3$) δ 1.76 (s, 6H), 1.97 (s, 6H), 4.06 (s, 4H), 6.60 (s, 2H); ^{13}C NMR (50 MHz, $CDCl_3$) δ 19.9, 20.5, 110.2, 114.6, 131.5, 136.1, 136.5, 142.8; MS (EI) m/z 400 (M + 4, 50), 398 (M + 2, 100), 396 (M+, 52), 117 (51), 111 (89); HRMS (EI) calcd for $C_{16}H_{18}Br_2N_2$: 395.9837. Found: 395.9842.

(±)-3,3′-Dibromo-4,4′-dihydroxy-2,2′,6,6′-tetramethylbiphenyl ((±)-15). The procedure described for the synthesis of **(±)-10** was followed using **(±)-14** (0.1 g, 0.25 mmol) as the starting material. Purification by Kugelrohr distillation (0.06 Torr, 50 °C) gave 93 mg (92%) of **(±)-15** a colorless oil: ^{1}H NMR (200 MHz, $CDCl_3$) δ 1.81 (s, 6H), 1.99 (s, 6H), 5.63 (s, 2H), 6.86 (s, 2H); ^{13}C NMR (50 MHz, $CDCl_3$) δ 19.9, 20.3, 111.1, 114.7, 132.6, 136.1, 136.9, 151.1; MS (EI) m/z 402 (M + 4, 1), 400 (M + 2, 1), 398 (M+, 1), 281 (2), 225 (2), 221 (3), 207 (5), 167 (7), 149 (44), 147 (11), 123 (20), 111 (27), 109 (25); HRMS (EI) calcd for $C_{16}H_{16}O_2N_2$: 397.9517. Found: 397.9531.

(+)-3,3′-Dibromo-2,2′,6,6′-tetramethyl-4,4′- bis[(4-*n*-nonyloxybenzoyl)oxy]biphenyl ((+)-4). The procedure described for the synthesis of **(−)-2** was followed using **(±)-15** (0.163 g, 0.41 mmol) to give 0.22 g (60%) of **(±)-4** as a white solid. The product was resolved by chiral-phase HPLC using a Regis (*S,S*)-Whelk-O1 column (93:7 hexanes/$CHCl_3$, 5 mL/min). The first eluant was collected and concentrated and the residue was recrystallized from hexanes after filtration through a 0.45-μm PTFE filter to give **(+)-4** in optically pure form: mp 110−112 °C; $[\alpha]_D^{24}$ +2.48 (c 0.75, $CHCl_3$); ^{1}H NMR (200 MHz, $CDCl_3$) δ 0.89 (t, J = 5.6 Hz, 6H), 1.29−1.50 (m, 24H), 1.76−1.90 (m, 4H), 1.91 (s, 6H), 2.09 (s, 6H), 4.06 (t, J = 6.5 Hz, 4H), 7.00 (d, J = 8.8 Hz, 4H), 7.11 (s, 2H), 8.21 (d, J = 8.8 Hz, 4H); ^{13}C NMR (50 MHz, $CDCl_3$) δ 14.1, 19.9, 20.4, 22.7, 26.0, 29.1, 29.2, 29.3, 29.5, 31.9, 68.4, 114.4, 116.9, 121.2, 122.7, 132.5, 136.1, 137.3, 138.1, 147.7, 163.7, 164.2. Anal. Calcd for $C_{48}H_{60}Br_2O_6$: C, 64.57; H, 6.77; Br, 17.90. Found: C, 64.67; H, 6.67; Br, 18.17.

(−)-2,2′,3,3′,6,6′-Hexamethyl-4,4′-bis[(4-*n*-nonyloxybenzoyl)oxy]biphenyl ((−)-5). The racemic diol **(±)-16** was resolved by chiral-phase HPLC using a Daicel Chiralpak AS column (9:1 hexanes/EtOH, 3 mL/min). The procedure described for the synthesis of **(−)-2** was followed using **(−)-16** (second eluant collected, 13 mg, 0.05 mmol) to give 19 mg (51%) of **(−)-5** as a white solid: mp 124−126 °C; $[\alpha]_D^{25}$ −1.82 (c 1.4, $CHCl_3$); ^{1}H NMR (400 MHz, $CDCl_3$) (0.89 (t, J = 6.8 Hz, 6H), 1.29−1.50 (m, 24H), 1.80−1.88 (m, 4H), 1.88 (s, 6H), 1.89 (s, 6H), 2.15 (s, 6H), 4.05 (t, J = 6.6 Hz, 4H), 6.95 (s, 2H), 6.99 (d, J = 8.9 Hz, 4H), 8.18 (d, J = 8.9 Hz, 4H); ^{13}C NMR (100 MHz, $CDCl_3$) 13.0, 14.1, 16.6, 20.0, 22.6, 26.0, 29.1, 29.2, 29.3, 29.5, 31.8, 68.3, 114.3, 120.7, 121.7, 126.3 132.2 134.1, 136.1 137.8 148.2, 163.4, 164.9. Anal. Calcd for $C_{50}H_{66}O_6$: C, 78.70; H, 8.72. Found: C, 78.72; H, 8.59.

Ferroelectric Polarization and Helical Pitch Measurements. Texture analyses and transition temperature measurements for the doped liquid crystal mixtures were carried out using a Nikon Labophot-2 polarizing microscope fitted with a Instec HS1-i hot stage. Spontaneous polarizations (P_S) were measured as a function of temperature by the triangular wave method[14] (6 V/μm, 80−100 Hz) using a Displaytech APT-III polarization testbed in conjunction with the Instec hot stage. For each data point taken, the temperature of the sample was allowed to fully equilibrate to rule out any temperature effect during measurement. Polyimide-coated ITO glass cells (4 μm × 0.25 cm^2) supplied by Displaytech Inc. (Longmont, CO) were used for all the measurements. Good alignment was obtained by slow cooling of the filled cells from the isotropic phase via the N* and SmA* phases. Tilt angles (θ) were measured as a function of temperature between crossed polarizers as half the rotation between two extinction positions corresponding to opposite polarization orientations. The sign of P_S along the polar axis was assigned from the relative configuration of the electrical field and the switching position of the sample according to the established convention.[3] Measurements of SmC* helical pitch were carried out at $T - T_C = -10$ K on a 150-μm film of the liquid crystal material in a planar alignment using a Nikon Labophot-2 polarizing microscope fitted with a Instec HS1-i hot stage. The helical pitch was measured as the distance between dark fringes caused by the periodicity of the SmC* helix.[27]

Acknowledgment. We are grateful to the Natural Sciences and Engineering Research Council of Canada, the Canada Foundation for Innovation, the Ontario Challenge Fund, and the Ferroelectric Liquid Crystal Materials Research Center (National Foundation MRSEC Award DMR-9809555) for financial support of this work.

CM000753K

(27) Martinot-Lagarde, P. *J. Phys.* **1976**, *C3*, 129.